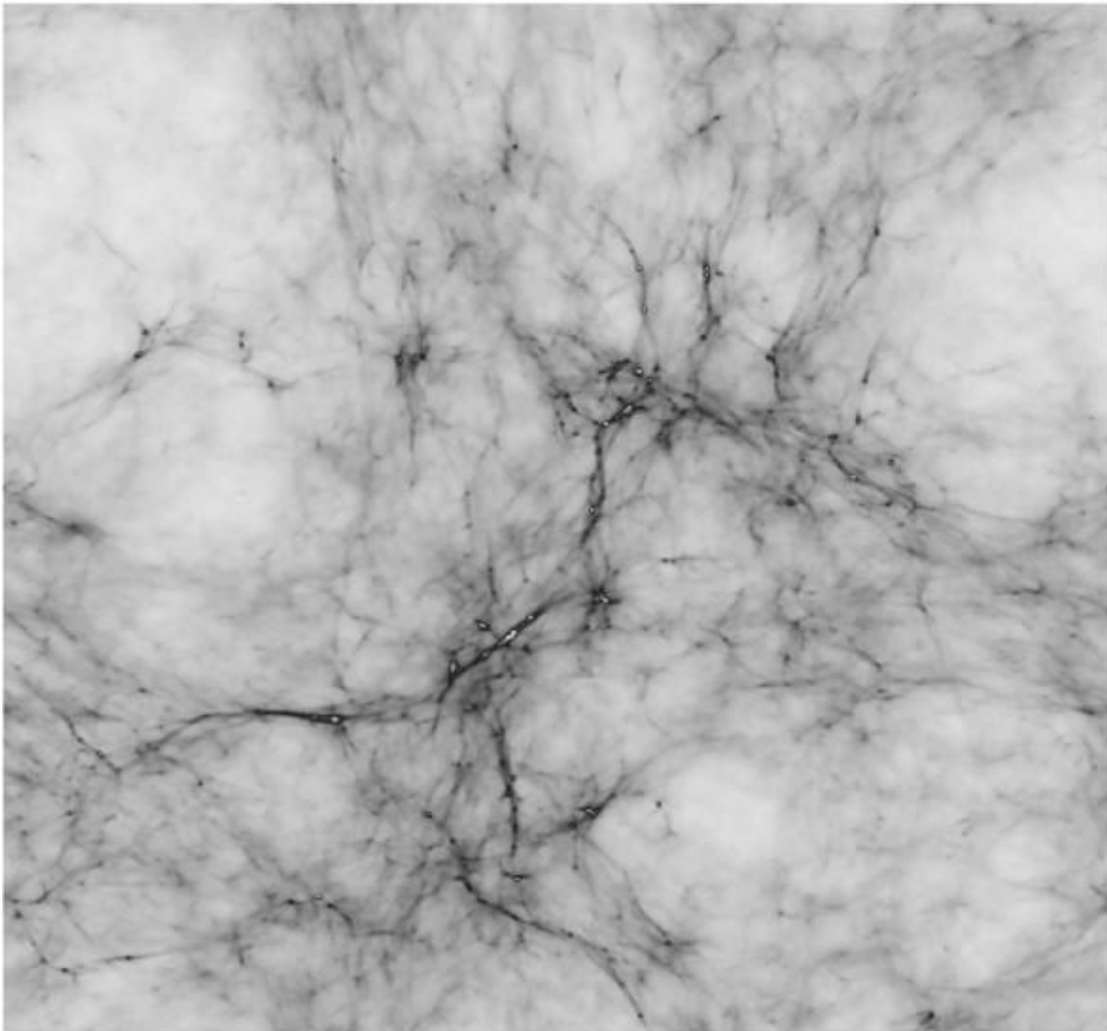


# Enrichment by Population III stars

Arjen Siegers, [siegers@astro.rug.nl](mailto:siegers@astro.rug.nl)  
Supervisor: Marco Spaans

August 19, 2004



# 1 Introduction

This is the report of my Klein Onderzoek, which I conducted under supervision of Marco Spaans (Kapteyn Astronomical Institute).

The aim of this project was to investigate the enrichment caused by the first stars. These stars are known as Population III, as a logical continuation of the Population I and II currently found in stellar systems.

In the Big Bang scenario, the first nucleosynthesis takes place in the first 15 minutes. During this time only hydrogen, helium and some trace elements such as deuterium, tritium, lithium and beryllium are formed. During the epoch of primordial nucleosynthesis matter and radiation are coupled, and the entire universe is ionized. When they decouple, the universe becomes neutral, i.e., the electrons combine with the nuclei, and the photons that are emitted during this process create the background radiation. This happens at a redshift of  $\sim 1000$ . After recombination the universe cools, and the radiation field shifts from optical to infrared, in other words, the universe goes dark. Finally, at a redshift between 20 and 15, matter contracted and formed the first stars, thus lighting up the universe and beginning the epoch of reionization.

Because the matter in which these stars formed is metal-free, its cooling characteristics are radically different from that of the gas in which modern stars (Population I and II) have formed. The only

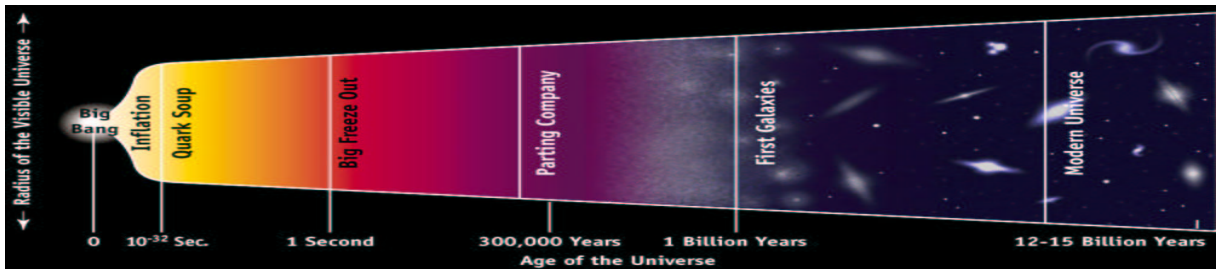


Figure 1: The evolution of the Universe according to the current Big Bang model. The first star formation takes place around  $z \sim 20$ , or around an age of  $\approx 100$  million years in this figure.

available mechanism for cooling are the rotational and vibrational transitions of the hydrogen molecule. In the current epoch molecular hydrogen is formed on dust particles. However, the primordial gas is dust-free, so the molecular hydrogen has to form through the far less effective gas phase route.

As a result of the less effective cooling, the fragments have a much higher temperature than in present-day star formation, so their Jeans mass is much higher. The resulting stars are generally expected to be much heavier than present-day stars.

Because of their greater mass, Population III stars are expected to have a rather short lifetime ( $\sim 10^6$  yr). The way in which massive, metal-free stars end their lives depends largely on their initial mass (Heger et al. 2003). For an initial mass of  $9-25M_{\odot}$  they produce a neutron star, while above  $25M_{\odot}$  they produce black holes, with one exception. In the mass band  $140-260 M_{\odot}$ , they end their existence in pair instability supernovae. This is an extremely powerful process in which part of the gas energy in the star is converted to the rest mass of electron-positron pairs which cause sudden loss of pressure in the star. This results in implosive oxygen and silicon burning, which produce enough energy to reverse the collapse. This mechanism is powerful enough to completely disrupt the star, leaving no remnant (Heger and Woosley 2002). This is one of the models that is investigated in this report.

The other process that could be responsible for the early enrichment that will be discussed is the hypernova model as proposed by Umeda and Nomoto(2002). This involves core collapse supernovae of stars in the mass range  $25 - 35M_{\odot}$  with explosion energies of the order of  $10^{52}$  ergs (Nomoto et al. 2002).

Although it is highly unlikely that we observe Population III stars directly, their enrichment signatures can probably be found in extremely metal poor( $Z < 10^{-3}Z_{\odot}$ ) stars in the galactic halo

(Scannapieco et al. 2003). In this report recent observations by Cayrel et al.(2004) will be used to test the pair instability and hypernovae models. This report is set up as follows: §2 will treat the formation of the Population III stars and their initial mass function. §3 and §4 will treat the pair instability supernovae and the hypernovae, respectively. In §5 the models will be compared to observations of extremely metal poor stars in the galactic halo. Finally, in §6 the conclusions are presented and discussed.

## 2 Population III: Formation and Initial Mass Function

The first stars are formed from metal-free gas, which has been produced in the nucleosynthesis immediately following the Big Bang. This gas consists mostly of hydrogen and helium. Due to small irregularities (anisotropies) in the density of the early universe, gravitational collapse will cause the formation of clumps in the gas. In these clumps further collapse will lead to the creation of the first stars.

When these clouds collapse, the temperature increases due to shock heating to temperatures above  $10^3$  K (Nakamura & Umemura 2001). When we apply the virial theorem we find  $2E_{thermal} = -U$ , where  $E_{thermal} = N_H kT$ . The gravitational potential energy of the cloud is (Zeilik et al. 1998):

$$U \approx \frac{-GMm}{R} \approx -GM^2/L.$$

This is a self-gravitating system and  $L$  is the size scale of the collapsing region. The initial cloud consists mostly of atomic hydrogen, so  $N = M/m_H$ . Thus, the virial theorem gives:

$$2(M/m_H)kT \approx GM^2/L$$

$$2kT/m_H \approx GM/L.$$

So the mass of the collapsing region will be proportional to its temperature. The critical mass for gravitational collapse with an external pressure  $P_{ext}$  is given by the Ebert and Bonnor mass:

$$M_{BE} = 1.18M_{\odot}(c_s^4/G^{3/2})P_{ext}^{-1/2} \quad (1)$$

$$c_s^2 = dP/d\rho = \gamma k_B T / \mu m_H. \quad (2)$$

By taking the internal equal to the external pressure, Abel et al. (2002) get  $M_{BE} \approx 20M_{\odot}T^{3/2}n^{-1/2}\mu^{-2}\gamma^2$ , where  $n$  is the particle number density and  $\mu \approx 1.22$  is the mean mass per particle in terms of the proton mass. For the adiabatic index  $\gamma = 5/3$  is used. For a temperature of 1000K, this would result in a  $M_{BE} \approx 10^6 M_{\odot}$ , so it is necessary for the gas to cool to form objects of the order of a stellar mass.

Atomic hydrogen is only effective for cooling at  $T > 10^4$ K, below this temperature cooling through rotational and vibrational transitions of  $H_2$  takes over (Schneider et al. 2002).

In the present day universe, molecular hydrogen forms on the surfaces of dust grains. The pristine gas in which the first stars form is completely dust-free, so the  $H_2$  has to form in another way. Molecular hydrogen can be found through the gas reaction (Nakamura and Umemura 1999),



and:



The cooling by  $H_2$  takes the gas to characteristic values  $T_c \sim 200K$  and  $n_c \sim 10^4 \text{cm}^{-3}$ . This is a

quasi-hydrostatic state, and is more generally referred to as a 'loitering phase'. During this phase the gas undergoes a slow contraction. When enough mass has been accumulated to exceed the Jeans mass, which is  $\sim 10^3 M_\odot$  at the characteristic values for the temperature and the density, the gas becomes gravitationally unstable and the temperature rises again, to  $T \sim 1000K$ , but this is not enough to stop the collapse (Bromm et al. 2002). As the density increases to  $n \gtrsim 10^8 cm^{-3}$ , it is also possible to form molecular hydrogen through three-body reactions (Nakamura and Umemura 1999, Bromm 2004):



and:



At one time during the collapse a hydrostatic cloud is formed with a mass of  $\sim 5 \times 10^{-3} M_\odot$  (Omukai & Nishi 1998). The mass of the protostar is then limited only by the amount of matter that can accrete onto this core. The accretion has been studied in detail by Omukai & Palla (2001, 2003). Before the temperature is high enough to start hydrogen burning the accretion is limited by the Eddington limit<sup>1</sup>, and only the accretion causes any radiation. Thus, with  $L_{tot} \sim L_{acc} \simeq GM_* \dot{M}_{acc} / R_*$ , the limiting case is  $L_{acc} \simeq L_{Edd}$ . So we can write the critical accretion rate as:

$$\dot{M}_{crit} \simeq \frac{L_{Edd} R_*}{GM_*} \sim 5 \times 10^{-3} M_\odot yr^{-1}, \quad (9)$$

where  $R \sim 5R_\odot$ , which is a typical value for Population III stars (Bromm 2004). A large unknown in our knowledge of the accretion of matter onto the protostellar core is the process which terminates the accretion phase (Tan & McKee 2004). One of the problems here is that the accreting matter forms a disk around the protostar, while photons are being radiated in all directions. Thus, only a very small portion of the photons will do work on the infalling matter, and will not stop the accretion. Then the only limiting factor on the maximum size of the star is the amount of available gas. Currently it is thought that the accretion phase ended either by the formation of an HII region in the accretion region around the protostar (Omukai & Inutsuka 2002) or by radiation pressure exerted by trapped Ly $\alpha$  photons (Tan & McKee 2002).

Because of the uncertainty in the accretion process, a large range of masses has been proposed. Nakamura and Umemura (2001) find a bimodal IMF as shown in figure 2. Also shown in this figure are the mass ranges for which enrichment is possible. These mass ranges will be investigated in some detail later on.

### 3 Pair instability supernovae

There are several ways in which massive, metal poor stars can end their lives, depending on their exact metallicity and their initial mass (Heger et al. 2003). As figure 3 (figure 1 from Heger et al. 2003) shows, most of the massive stars ( $M \geq 9M_\odot$ ) end up either as neutron stars or as black holes. At solar metallicity, very massive stars ( $M > 100M_\odot$ ) undergo nuclear-powered and opacity-driven pulsations that increase the mass loss. However, at zero metallicity, both these effects cause a mass loss of the order of  $1 M_\odot$  (Baraffe et al. 2001) which constitutes about 1% of the total mass, so mass loss can be safely ignored.

Massive metal free stars heavier than  $\sim 100M_\odot$  encounter pulsations caused by the pair instability (Heger et al. 2003). The pair-instability is the process whereby energy that could have increased the temperature or provide pressure support is converted into electron-positron pairs (Heger and Woosley 2002):

$$\gamma \rightarrow e^- + e^+,$$

---

<sup>1</sup>The Eddington limit, or Eddington luminosity is the luminosity at which radiation pressure becomes high enough to stop gravitational contraction

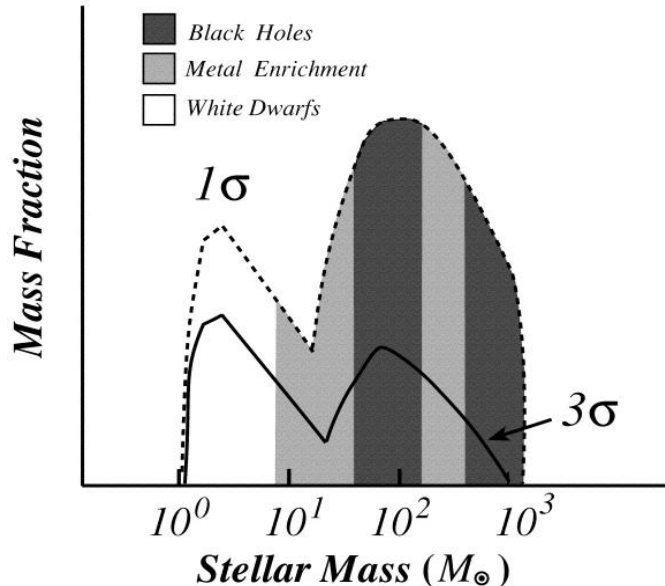


Figure 2: The bimodal initial mass function as found by Nakamura and Umemura(2001). The  $1\sigma$  and  $3\sigma$  denote the mass fluctuations in which the Pop III stars formed.

which annihilate to form a neutrino and an anti-neutrino (Fowler & Hoyle 1964):

$$e^- + e^+ \rightarrow \nu + \bar{\nu}.$$

This causes the pressure to drop, and the outer layers drop in onto the core, which results in an increase in temperature and pressure, and eventually nuclear burning causes an energetic explosion with energies of the order of  $10^{51}$  erg. When a star has  $M < 140M_\odot$  this leads to strong pulsations, since the explosions are not energetically enough to explode the entire star. When a star is  $140M_\odot < M < 260M_\odot$ , the star is completely disrupted (Heger & Woosley 2002). The pair instability supernova process is significant in that it is the only way for massive metal poor stars to enrich their environment. It has been speculated that the IMF of these stars would have been extremely top-heavy (e.g. Ripamonti et al. 2002, Bromm et al. 2002), and stars with masses  $> 260M_\odot$  create black holes which are massive enough to make it impossible for the expelled matter to escape their potential well. So, if such an IMF is assumed for the Population III, the pair instability supernova would be the only model to enrich the universe.

## 4 Hypernovae

The hypernova model was proposed by Umeda and Nomoto (e.g., Umeda & Nomoto 2002, hereafter: UN02). They propose high energy( $E_{kin} \sim 10^{52}$  erg, which is about ten times more powerful than a regular Type II SNe) supernovae to account for the abundance patterns as found in the extremely metal poor stars in the galactic halo.

At low metallicities, some authors have found that  $[Zn/Fe]^2$  increases with decreasing metallicity,  $[Fe/H] \lesssim 3$ . UN02 tried to explain this with enrichment by type II supernovae. The initial mass range is here  $20M_\odot \leq M_{init} \leq 35M_\odot$ . In their 2002 article, Umeda & Nomoto investigate the nucleosynthesis of Zn and the iron peak elements. They discuss models using stars in a mass range of  $13M_\odot \leq M_{init} \leq 30M_\odot$ , and a range in explosive energies from  $E_{51}^3 = 1$  to  $E_{51} = 50$ .

<sup>2</sup>The notation of the form  $[A/B]$  denotes:  $[A/B] \equiv \log_{10}(A/B) - \log_{10}(A/B)_\odot$

<sup>3</sup> $E_{51} = 1 \times 10^{51}$ erg

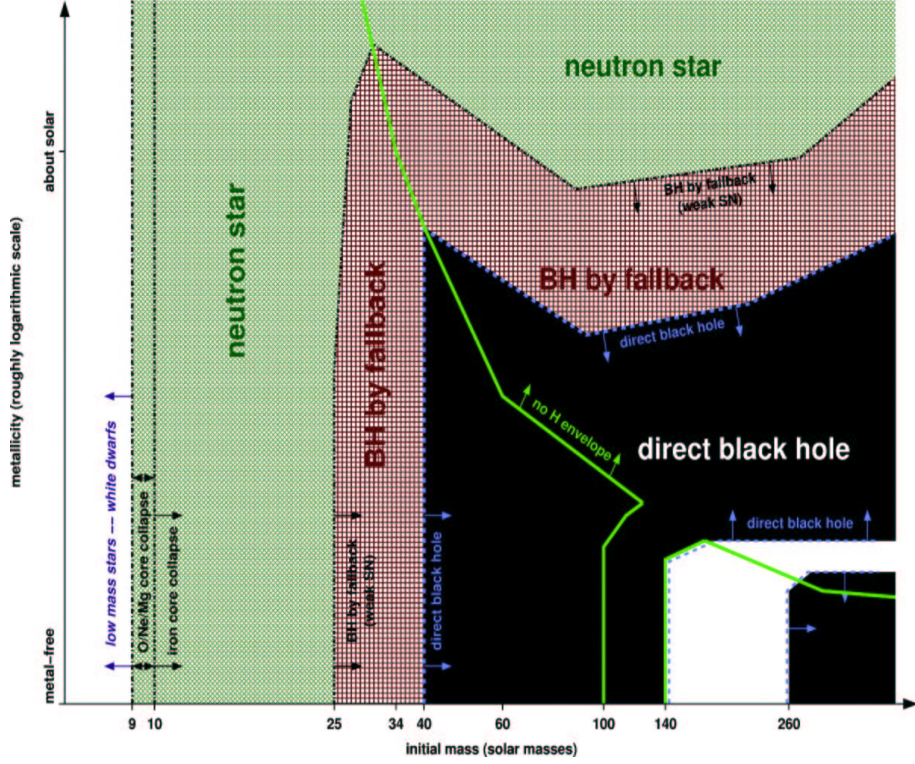


Figure 3: This figure shows the ultimate fate of massive stars depending on their metallicity and initial mass.

They investigate every explosion energy, and find that the relative abundance of  $[Zn/Fe]$  which they are looking for requires  $E_{51} \gtrsim 2$  for stars with a mass  $M \sim 13M_{\odot}$  to  $E_{51} \gtrsim 20$  for stars with  $M \gtrsim 20M_{\odot}$ . They focus on the  $[Zn/Fe]$ , since this is very important for studying the abundance patterns of damped Ly $\alpha$  systems.

They find that two models are the most probable: 1. Hypernova-like explosions of massive stars ( $M \leq 25M_{\odot}$ ) with  $E_{51} > 10$  and 2. Explosions of less massive stars ( $M \leq 13M_{\odot}$ ) with  $E_{52} \geq 2$ . The models for the hypernovae are much more complex than those for the pair instability supernovae. While the pair instability supernova depends largely on the initial mass and metallicity of the progenitor, a lot more parameters are available for 'tweaking' in the hypernova model. UN02 investigate specifically the dependence of Zn on the following parameters: the mass cut<sup>4</sup>,  $M_{cut}$ , the dependence on total stellar mass, the dependence on  $Y_e$  (the number of electrons per baryon), the explosion energy of the supernova and the effects of mixing and fallback. In their final results, they pick fixed values for all these variables except for the explosion energy and the initial stellar mass.

## 5 Stellar Data

The data on the extremely metal poor halo stars was taken from Cayrel et al (2004). Cayrel et al. have performed these observations using the VLT-UT2 and the high-resolution spectrograph UVES. Those stars listed with a CSXXXX-XX number can be found online in SIMBAD using BPS CSXXXX-XX names. In the article, 35 stars are analyzed. Of these, 30 are in the metallicity range  $-2.7 < [Fe/H] < -4.1$ . From these, I have selected a broad sample, in order to cover

<sup>4</sup>The mass cut is the radial mass ( $M_r = M_{cut}$ ) at which the ejecta and the remnant of the supernova are separated

the entire range of metallicities, with an emphasis on stars with  $[\text{Fe}/\text{H}] \lesssim -3.0$ .

Name	$[\text{Fe}/\text{H}]$
HD 2796	-2.47
BD-18:550	-3.06
CD-38:245	-4.19
BD+17:3248	-2.07
BS16467-062	-3.77
CS22189-009	-3.49
CS22885-096	-3.78
CS22896-154	-2.69
CS22949-037	-3.97
CS22956-050	-3.33

Table 1: The stars used in this report with their respective metallicities.

On a number of elements which are featured in the models, no observational data was available. In the processing of the data I have set these equal to zero. A large spread in the data is obvious, both in the  $[\text{Fe}/\text{H}]$  as in the other abundances (see table 1 and table 2).

## 6 Comparison and results

The objective of this research project was to produce a yield of heavy elements as produced by a Nakamura and Umemura type IMF. This yield was to be produced by weighing the hypernovae and pair instability supernovae models according to this IMF.

Data for the abundance patterns from the pair instability supernova have been taken from Heger & Woosley (2002). In this paper they give the abundance patterns for 15 Population III stars (that is, stars with zero metallicity at the time they are formed) over the entire initial mass range  $140 - 260M_{\odot}$ .

The data used for the hypernova model has been taken from Umeda and Nomoto (2002). They have produced models of stars in the range  $13\text{-}30 M_{\odot}$  and with explosion energies ranging from  $E_{51} = 1$  to  $E_{51} = 50$ .

I have decided to look only at the elements in the range C-Zn. These were available for both models and for the observed halo stars. In table 3 the convention is listed which will be used to denote the different species.

**PISN data** The data in HW02 were expressed in terms of production factors. The production factor,  $P_i$ , is defined as the mass fraction of a given species in the ejecta of the PISN compared to its mass fraction in the sun:

$$P_i = \frac{M_X/M_{tot}}{M_{X,\odot}/M_{tot,\odot}}$$

This relates to the normal abundance parameter  $[X/Fe]$  as follows:

$$[X/Fe] = \log_{10}(X/Fe) - \log_{10}(X_{\odot}/Fe_{\odot}) = \log_{10} \left( \frac{X/Fe}{X_{\odot}/Fe_{\odot}} \right). \quad (10)$$

**Hypernova data** The data for the hypernova model were listed as total mass in the ejecta after radioactive decay. This data was put into the form  $[X/Fe]$  by using equation 10. The solar values for the abundances were taken from Grevesse and Sauval (1998) (See figure 6).

Name	C	N	O	Na	Mg	Al	Si	K	Ca	Sc	TiI	TiII	Cr	Mn	Fe I	Fe II	Co	Ni	Zn
HD 2796	-0.51	-	0.50	0.34	0.25	-0.66	0.40	0.60	0.32	0.09	0.20	0.24	-0.26	-0.39	0.01	-0.02	0.14	-0.09	0.24
BD-18:550	-0.02	-	0.42	0.05	0.31	-0.59	0.39	0.52	0.41	0.04	0.16	0.14	-0.34	-0.38	0.00	0.00	0.19	-0.05	0.22
CD-38:245	< -0.33	-	-	-0.06	0.20	-0.67	0.20	-	0.20	0.04	0.37	0.25	-0.44	-0.60	-0.01	0.02	0.37	-0.19	0.69
BD+17:3248	-0.44	0.57	0.69	0.69	0.19	-0.71	0.52	0.82	0.40	0.20	0.23	0.33	-0.22	-0.47	0.02	-0.03	0.36	0.00	0.00
BS16467-062	0.25	-	-	-0.17	0.16	-0.90	0.42	0.43	0.35	0.01	0.40	0.18	-0.41	-0.55	-0.06	0.06	0.55	0.08	0.23
CS22189-009	0.27	-	-	-0.30	0.11	-0.92	0.29	0.40	0.20	0.00	0.13	0.04	-0.42	-0.25	0.00	0.00	0.37	0.06	0.46
CS22885-096	0.24	-	-	-0.06	0.19	-0.79	0.52	0.34	0.35	0.37	0.34	0.32	-0.48	-0.54	-0.03	0.03	0.48	0.00	0.44
CS22896-154	0.27	-	0.94	0.12	0.08	-0.76	0.54	0.45	0.36	0.13	0.27	0.33	-0.23	-0.59	0.01	0.00	0.38	-0.05	0.26
CS22949-037	1.17	2.57	1.98	1.44	1.56	-0.17	0.77	0.23	0.34	0.09	0.35	0.36	-0.42	-0.47	-0.03	0.02	0.33	-0.10	0.66
CS22956-050	0.28	-	-	-	0.37	-0.65	0.78	0.29	0.46	-0.04	0.35	0.29	-0.34	-0.51	0.01	-0.01	0.39	0.01	0.30

Table 2: The abundances for the stars as taken from Cayrel et al (2004). The abundances are in the form  $[X/Fe]$ , as defined before.

No.	Element	No.	Element
0	C	13	K
1	N	14	Ca
2	O	15	Sc
3	F	16	Ti
4	Ne	17	V
5	Na	18	Cr
6	Mg	19	Mn
7	Al	20	Fe
8	Si	21	Co
9	P	22	Ni
10	S	23	Cu
11	Cl	24	Zn
12	Ar		

Table 3: Indices associated with species, as used in the plots in this section.

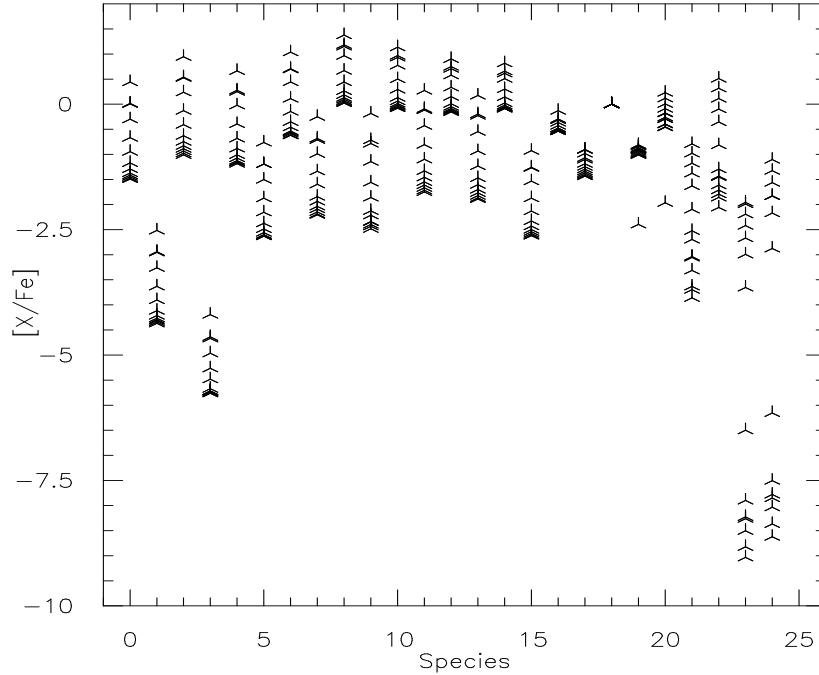


Figure 4: The abundance pattern for the entire mass range ( $140\text{-}260M_{\odot}$ ) of the pair instability supernova model.

**Stellar data** The stellar data were already in the form  $[X/Fe]$ . However, not all the elements which are predicted in the model are measured, so the files containing the stellar data had to be matched to the models. This was done by inserting zeroes in the file for those elements on which no data was available. Also, for Fe and Ti abundances of various ionization levels were measured. These were added to obtain the total abundance of the element.

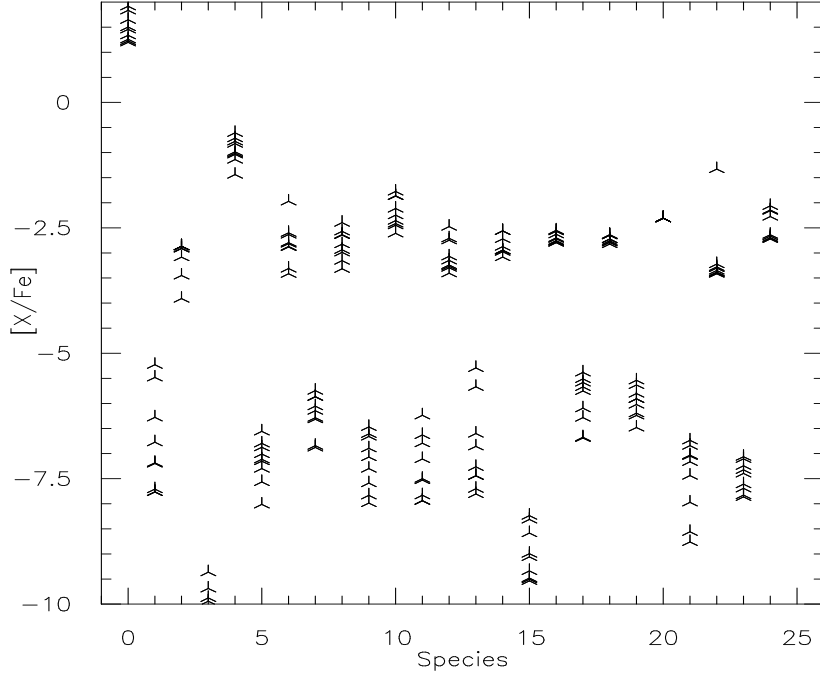


Figure 5: The abundance pattern for hypernovae with all masses and explosion energies as investigated.

**Initial Mass Function** Finally, the data from the observations were compared to the initial mass function as proposed by Nakamura & Umemura (2001) (see also fig.2). This is a bimodal function:

$$\frac{dN}{d \log m} = \frac{(dN_{low} + dN_{high})}{d \log m}, \quad (11)$$

where

$$\frac{dN_{low}}{d \log m} = \begin{cases} Am^{-\alpha} & \text{for } m \geq m_{p1}, \\ 0 & \text{for } m < m_{p1}, \end{cases} \quad (12)$$

$$\frac{dN_{high}}{d \log m} = \begin{cases} Bm^{-\beta} & \text{for } m \geq m_{p2}, \\ 0 & \text{for } m < m_{p2}, \end{cases} \quad (13)$$

where  $m_{p1}$  and  $m_{p2}$  are the masses at which the peaks in the IMF are located. Values are:  $m_{p1} \sim 1M_{\odot}$  and  $m_{p2} \sim 10 - 10^2 M_{\odot}$  and:

$$A \sim (\alpha - 1)\kappa\epsilon M_{total} m_{p1}^{\alpha-1} \quad (14)$$

$$B \sim (\beta - 1)(1 - \kappa)\epsilon M_{total} m_{p2}^{\beta-1}. \quad (15)$$

In these equations,  $M_{total}$  is the total mass of the cloud in which the star forms,  $\alpha$  and  $\beta$  are the slope of the first and second peak in the IMF respectively, and  $\epsilon$  is the efficiency of the star formation in the cloud.

**Method** To compare the models with the observations, the initial mass function (eq.11 through 13) was evaluated for all mass ranges that can enrich the primordial gas. This was used to weigh the abundance patterns produced by each combination of model, mass and (in the case of the hypernova model) explosion energy. The various explosion energies in the hypernova model were

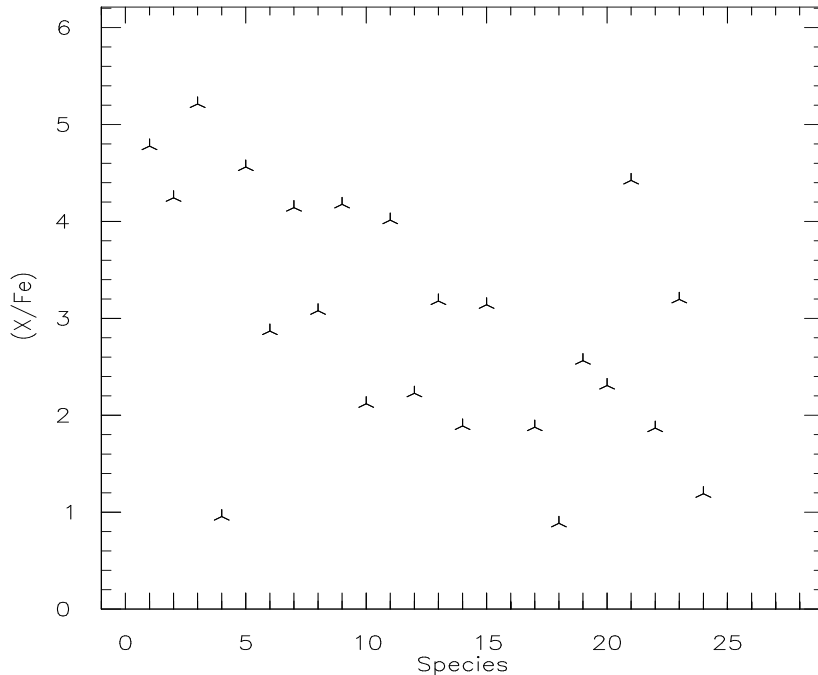


Figure 6: The solar abundance pattern as used to reduce the data from the hypernova model (Grevesse & Sauval 1998)

given equal weights, thus assuming they are equally probable. This is justified because Umeda and Nomoto use the energy as an input parameter, and do not give any preference for the occurrence of supernovae with a certain energy over another energy.

Since the stellar data do not cover the same range of species as the models, some of the abundances have been set equal to zero. These are: O, F, Ne, Cl, Ar, V, Cu.

In figure 7, I plot the abundance patterns for three of the stars from the sample. These are BD+17:3248 (red stars), CD-38:245 (green stars) and BD-18:550 (blue stars). These were selected because they have the highest, lowest and an intermediate value for  $[\text{Fe}/\text{H}]$ , respectively. The predicted abundance for a Nakamura and Umemura IMF is shown, with  $\alpha = \beta = 1.35$ ,  $\epsilon = 0.01$ ,  $M_{\text{tot}} = 10^7 M_{\odot}$ , the first peak at  $m_{p1} = 1.0 M_{\odot}$  and the second peak at  $m_{p2} = 100 M_{\odot}$ . Figure 8 shows the same, but here with a  $\alpha = \beta = 3.0$ .

## 7 Conclusions and discussion

From the plots in figures 6 and 7 it can be concluded that there is not much of a match between the models and the abundance patterns in the extremely metal poor stars in the halo of our galaxy. There are several explanations for this, some of which overlap.

First, the Population II stars in the galactic halo are assumed to be only the second generation of stars to have formed in the universe. This means that in their history they may have picked up all kinds of enrichment, for example when their orbits have taken them through the galactic disk. This idea is supported by the lack of a correlation between the value of  $[\text{Fe}/\text{H}]$  and the spread in their abundance patterns. That is, for a higher metallicity we do not see a higher general abundance pattern. This is illustrated in figures 7 and 8. In these figures, the trend in the  $[\text{Fe}/\text{H}]$

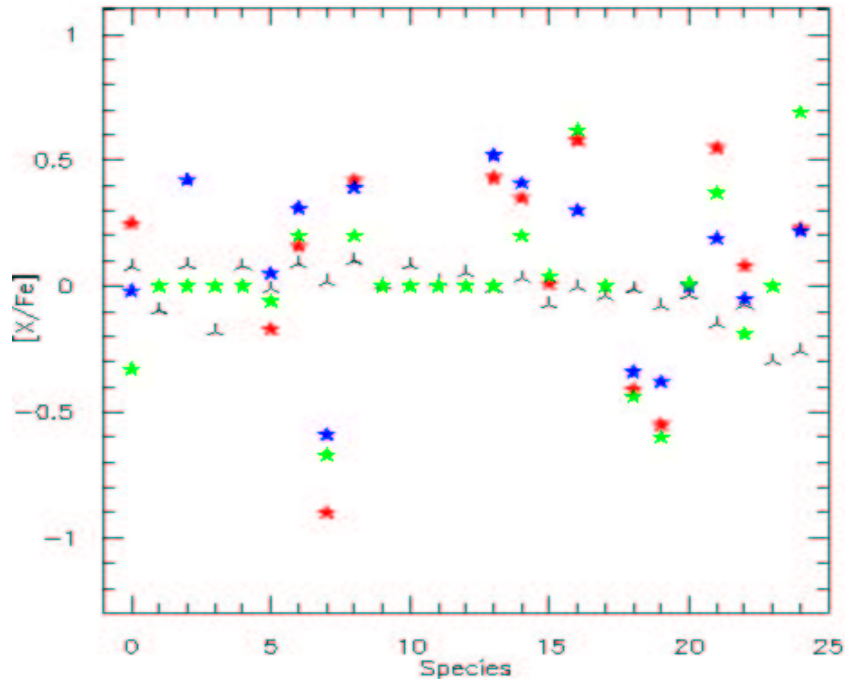


Figure 7: Abundance patterns from BD+17:3248(red)( $[\text{Fe}/\text{H}] = -2.07$ ), BD-18:550(blue)( $[\text{Fe}/\text{H}] = -3.06$ ) and CD-38:245(green)( $[\text{Fe}/\text{H}] = -4.19$ ) combined with the yield from a Nakamura and Umemura IMF with  $\alpha = \beta = 1.35$

values is not reflected in Na, Mg and Al. The star with the highest metallicity shows the lowest  $[\text{X}/\text{Fe}]$  value for these stars. This irregular pattern is repeated for almost all elements which have been measured. Only C and Ni show the expected sequence. Also, the size of the spread shows some dramatic differences. While the spread for Cr is only on the order of  $\sim 0.2$ , the spread in C is on the order of 1.0.

Second, three different theoretical models have been tested in this project: (1) The pair-instability model, (2) the hypernova model and (3) the IMF by Nakamura and Umemura. In all three of these models uncertainties are most probably present. Since star formation is still a largely unknown process, even in the present day universe, it would be very difficult to put forward an IMF which would result from a process that has never been observed.

There are alternatives to the approach using the halo stars however: Scannapieco et al. (2003) suggest the detection of the abundance patterns of the IGM itself through the Ly $\alpha$ -forest, but this is still limited to only a few elements. Also, searches in the ICM may give a good view of the enrichment by Population III stars. Finally, Scannapieco et al. (2003) propose the direct observation of Population III stars due to the fact that local Pop III star formation may have taken place fairly recently due to the very inhomogeneous spread of the enrichment throughout the universe.

## 8 Acknowledgements

I would like to thank Marco Spaans for the supportive and friendly way in which he guided me through this project.

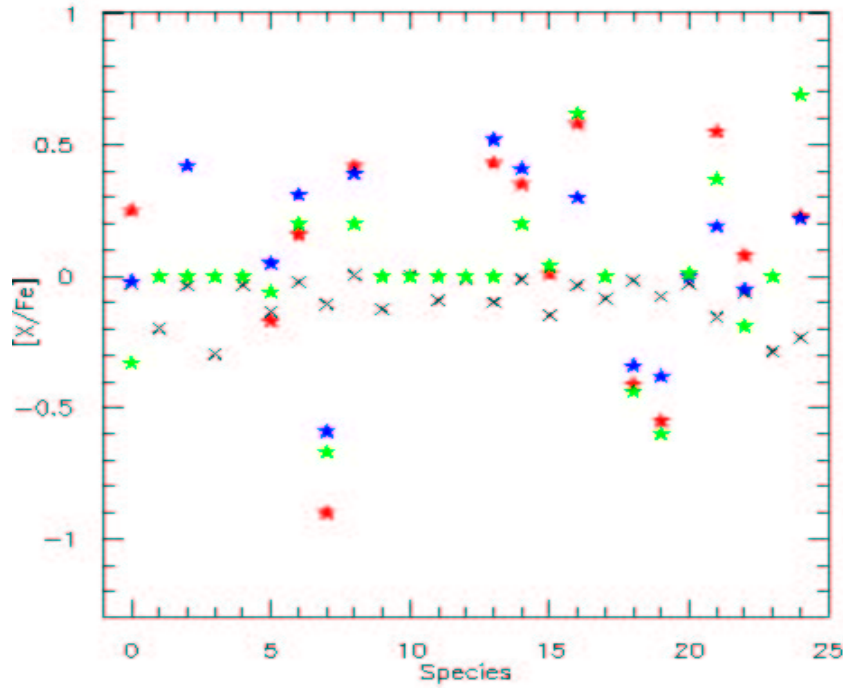


Figure 8: Abundance patterns from BD+17:3248(red)( $[\text{Fe}/\text{H}] = -2.07$ ), BD-18:550(blue)( $[\text{Fe}/\text{H}] = -3.06$ ) and CD-38:245(green)( $[\text{Fe}/\text{H}] = -4.19$ ) combined with the yield from a Nakamura and Umemura IMF with  $\alpha = \beta = 3.0$

## 9 References

- Abel, T., Bryan, G.L., Norman, M.L., 2002, *Science*, 295, 93
- Baraffe, I., Heger, A., Woosley, S.E., 2001, *ApJ*, 550:890
- Bromm, V., Coppi, P.S., Larson, R.B., 2002, *ApJ*, 564:23
- Bromm, V., 2004, *PASP*, 116:103
- Cayrel, R., Depagne, E., Spite, M., Hill, V., Spite, F., Francois, P., Plez, B., Beers, T., Primas, T., Andersen, J., Barbay, B., Bonifacio, P., Molaro, P., Nordström, B., 2003, *submitted to A&A*(astro-ph/0311092)
- Christlieb, N., Gustafsson, B., Korn, A.J., Barklem, P.S., Beers, T.C., Bessell, M.S., 2004, *ApJ*, 603, 708.
- Fowler, W.A., Hoyle, F., 1964, *ApJS*, 9, 201
- Grevesse, N., Sauval, A.J., 1998, *Space Sci. Rev.* 85, 161
- Heger, A., Woosley, S.E., 2002, *ApJ*, 567:532
- Heger, A., Fryer, C.L., Woosley, S.E., Langer, N., Hartmann, D.H., 2003, *ApJ*, 591:288
- Nakamura, F., Umemura, M., 1999, *ApJ*, 515:239
- Nakamura, F., Umemura, M., 2001, *ApJ*, 548:19

- Nomoto, K., Maeda, K., Umeda, H., Ohkubo, T., Deng, J., Mazzali, P., 2002, Proceedings of IAU Symposium #212, eds. van der Hucht et al.
- Omukai, K., Nishi, R., 1998, ApJ, 508:141
- Omukai, K., Inustuka, S., 2002, MNRAS, 332, 59-64
- Scannapieco, E., Schneider, R., Ferrara, A., 2003, ApJ, 589:35
- Schneider, R., Ferrara, A., Natarajan, P., Omukai, K., 2002, ApJ, 571:30
- Tan, J.C., McKee, C.F., astro-ph/0212283
- Tan, J.C., McKee, C.F., 2004, ApJ, 603:383
- Umeda, H., Nomoto, K., 2002, ApJ, 565:385
- Zeilik, M., Gregory, S.A., 1998, Introductory astronomy and astrophysics, 4<sup>th</sup> ed., Saunders college publishing.